

Perturbed Panel Flutter: A Simple Model

Leon R. Sinay*

Laboratorio de Computacao Cientifica - CNPq, Rio de Janeiro, Brazil

and

Edward L. Reiss†

Northwestern University, Evanston, Ill.

The effects of small periodic disturbances on the response of a two-degree-of-freedom, nonconservative mechanical system are analyzed. The system is a simple model for panel flutter. The disturbance simulates the pressure fluctuations of a turbulent boundary layer on the panel. Asymptotic expansions of the solutions are obtained for small-amplitude disturbances. The qualitative features of the response depend on the prescribed variation of the disturbance frequency with the magnitude of the nonconservative applied force. The disturbance can induce a smooth transition to the fluttering states of the rods, or it may induce jump transitions. The results suggest a possible technique for delaying panel flutter by applying periodic forcing functions with appropriate frequencies.

I. Introduction

PANEL flutter is caused by the interaction of an elastic plate with fluid flowing over its surface. The flow is basically parallel to the plate's surface. At low flow velocities, the panel oscillates with small amplitudes. Experiments suggest that the plate is then responding to the random pressure fluctuations of its turbulent boundary layer. The amplitude of the response increases slowly as the flow velocity increases. It increases rapidly as the velocity exceeds a critical value. Then the plate oscillates approximately periodically in time, so that the influence of the random pressure fluctuations is small. The critical velocity is called the flutter speed, and the periodically oscillating state is called flutter. A response diagram illustrating these features is shown by the solid curve in Fig. 1. In an experiment, the response diagram is a discrete set of points.

The classical mathematical models of panel flutter ignore the turbulent boundary-layer fluctuations and other sources of noise. We refer to them as pure flutter problems. Because of their complexity, these problems have been studied primarily by numerical computation; see Ref. 1 for a review. The results of these computations suggest that pure flutter problems can be characterized mathematically as bifurcation problems.

The solutions of a typical bifurcation problem have the following properties. There is a distinguished parameter λ , called the bifurcation parameter, and a distinguished solution, called the basic solution, which exist for all values of λ . The stability of the basic solution is determined from the linearized bifurcation theory. The values of λ for which the linear theory has nontrivial solutions are bifurcation points of the basic state. The corresponding solutions of the linear theory are the bifurcation modes. The critical value λ_c is defined as the smallest bifurcation point. The basic state is stable (unstable) if $\lambda < \lambda_c$ ($\geq \lambda_c$). Furthermore, one or more solutions of the nonlinear bifurcation problem branch from each of the bifurcation points. They are the bifurcation states. If for λ near a bifurcation point, the bifurcation states exist only for values greater than (less than) the bifurcation point, then the bifurcations are called supercritical (subcritical). A response diagram for supercritical bifurcation is shown by the

dotted curve in Fig. 1. In panel flutter, these terms have the following interpretations. The parameter λ is a dynamic pressure that is proportional to the square of the flow velocity. The basic solution corresponds to the flat state of the panel. The bifurcation points and modes are called the flutter speeds and modes, respectively. Finally, λ_c is the critical flutter speed, and the bifurcation states are the flutter states.

Thus, bifurcation implies a sharp transition at $\lambda = \lambda_c$ from the basic state to a bifurcated state. However, as shown in Fig. 1, these sharp transitions are not observed in experiments (see, e.g., Refs. 1 and 2). It is believed that turbulent boundary-layer pressure fluctuations are responsible for the smooth transitions. To study the effects of these fluctuations, the classical mathematical models of panel flutter must be modified. We refer to them as perturbed problems. Several attempts to solve perturbed problems numerically are summarized in Ref. 1. Since the methods are numerical, it is difficult to determine the mathematical structure of the solutions and their dependence on the physical, geometric, and flow parameters of the problems.

To develop analytical techniques for investigating the effects of pressure fluctuations on panel flutter, and to obtain a deeper understanding of the response structure, the simple model problem shown in Fig. 2 is analyzed in this paper. It is a two-degree-of-freedom, nonconservative mechanical system. It consists of two rigid rods of the same length and mass. They are connected at a common pivot by a linear torsional spring. The lower rod is connected to a fixed pivot by another torsional spring with the same modulus. A frictional force acts at the common pivot. This force is proportional to the relative angular velocities of the two rods. The torsional springs and the frictional force simulate the flexural rigidity and the structural and fluid dynamic damping of the panel, respectively.

The system is deformed by a compressive follower force f whose direction is always coaxial to the upper rod. It is a nonconservative force that simulates the fluid dynamic forces that act on the surface of the panel. The specified time-dependent force $P(T)$ always acts horizontally, as shown in Fig. 2; hence, it is a conservative force. This force simulates the pressure fluctuations of the turbulent boundary layer. We assume that $P(T)$ is small, since it represents noise.

Previous studies of nonconservative mechanical systems have considered systems similar to the present model, but with $P \equiv 0$, (see, e.g., Refs. 3-5 and references given therein). The analysis of these systems have been restricted to the linearized equations of motion to obtain the critical value of the follower force.

Received Dec. 1, 1980; revision received March 30, 1981. Copyright © American Institute of Aeronautics and Astronautics, Inc., 1981. All rights reserved.

*Scientist.

†Professor, Dept. of Engineering Sciences and Applied Mathematics.

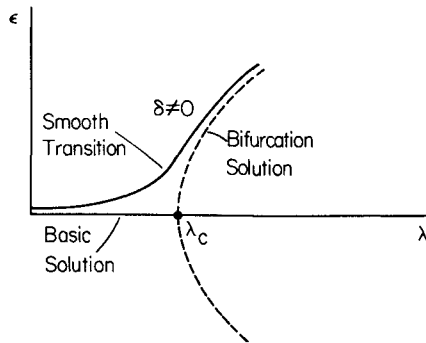


Fig. 1 The solid curve is a response diagram for panel flutter in the presence of turbulent boundary-layer pressure fluctuations. Here λ is a parameter which is proportional to the square of the flow velocity, and ϵ is an amplitude of the response of the panel. The dotted curve is a bifurcation, or flutter, state of the "pure" flutter problem (no turbulent boundary layer). The solution branches supercritically from the basic solution at the bifurcation point λ_c .

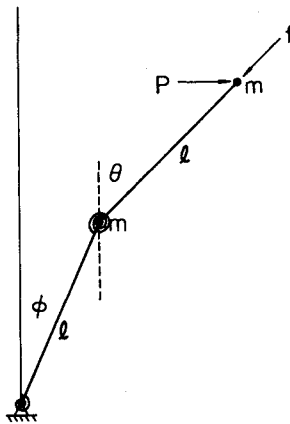


Fig. 2 Two-degree-of-freedom mechanical model.

The nonlinear equations of motion for this model are presented in Sec. II. They depend on three dimensionless parameters— λ , δ , and b . Here, λ is proportional to the follower force, δ is an amplitude of $P(T)$, and b is a dimensionless damping coefficient. When $\delta=0$, these equations define a bifurcation problem. Then the basic solution corresponds to the collinear, vertical state of the rods. This state is stable for $\lambda < \lambda_c$ and unstable for $\lambda \geq \lambda_c$, as shown in Sec. III. The Poincaré-Lindstedt perturbation⁶ method is used in Sec. IV to obtain the periodic solutions (flutter) that bifurcate supercritically from the basic state at $\lambda = \lambda_c$. The period of these solutions is denoted by $2\pi/\omega$, and it depends on λ .

The perturbed problem ($\delta \neq 0$), with $P(T)$ a periodic function of period $2\pi/\Omega$, is analyzed in Secs. V-VII. Since in panel flutter the pressure fluctuations depend on the flow velocity, we assume that Ω depends on λ . Furthermore, experiments suggest that for λ near λ_c the panel acts as a narrow bandpass filter. Thus, the response is nearly periodic with a frequency close to the natural frequency $\omega_0 = \omega(\lambda_c)$ of the panel. Thus, we assume that

$$\Omega(\lambda) = \omega_0 + w(\lambda - \lambda_c) + O((\lambda - \lambda_c)^2) \quad (1)$$

where w is a parameter. This is the resonance case of nonlinear vibration theory. The nonresonance case, $\Omega(\lambda_c) \neq \omega_0$, is not considered in this paper.

Asymptotic expansions of periodic solutions of period $2\pi/\Omega$ of the perturbed problem are obtained as $\delta \rightarrow 0$. A generalization of a previously developed method^{7,8} is used in the analysis. The generalization is necessary because the linearized bifurcation problem, evaluated at $\lambda = \lambda_c$, has two linearly independent solutions (two-dimensional null space), as shown in Sec. III. The previous analysis^{7,8} considers problems whose linearizations have only one independent solution at $\lambda = \lambda_c$. Although the generalization is slight, the results of the present analysis differ substantially from previous applications of the method.⁷⁻¹⁰

Because of the algebraic complexity, the length of the calculations, and because there have been several previous applications of the method, all details are omitted. However,

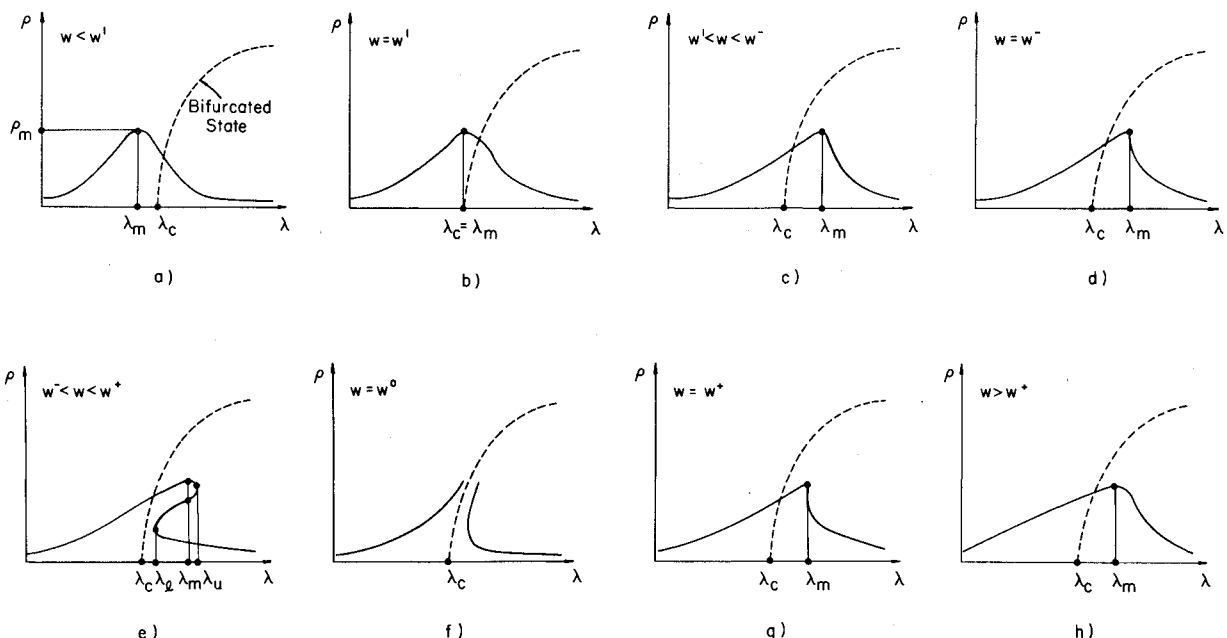


Fig. 3 Amplitude response curves for $q > 1$, where $\rho(\lambda)$ is the amplitude. The quantity w is the rate of change of the impressed frequency with λ at $\lambda = \lambda_c$. The dotted curve is the bifurcated (flutter) state.

a brief summary of the method is given in Sec. V. In addition, we have employed a computer symbolic manipulation language, ALTRAN,¹¹ to perform symbolically the algebraic manipulations of the perturbation and asymptotic methods used in Secs. IV and V.

The results are derived in Sec. VI, and are summarized in the response diagrams in Fig. 3. The smooth transition between the basic and bifurcated state, as shown in Fig. 1, is obtained only for the special value $w = w^0$ (see Fig. 3f). For this value of w , the frequencies of the forcing function, Eq. (1), and bifurcation states coincide to $O((\lambda - \lambda_c)^2)$. The other response diagrams in the figure suggest the existence of the critical values λ_m , λ_e , and λ_u , and the possibility of dynamic jumps to other states rather than a smooth transition. The results are discussed in Sec. VII. An alternate interpretation of the results is obtained by considering $P(T)$ as a deliberately imposed external force. Then the results suggest that flutter can be regulated by appropriately varying the frequency of the external force. More generally, the results suggest the use of periodic external forces as a nonlinear stability control method.

A more general mechanical system is analyzed in Ref. 12 using the same methods. Related results have been obtained for the hydrodynamic stability problem of plane Poiseuille flow with driven walls.¹³

II. Formulation

Referring to Fig. 2, dimensionless quantities are defined by

$$\tau \equiv (C/ml^2)^{1/2} T \quad x(\tau) = \theta(T) \quad y(\tau) = \phi(T) \\ b \equiv B[m\ell^2 C]^{-1/2} \quad \lambda = f\ell/C \quad \delta p(\tau) \equiv P(T) (\ell/C) \quad (2)$$

where m and ℓ are the mass and length of the rods, respectively; C and B are the moduli of the torsional springs and damping, respectively; T is time; and θ and ϕ are the rotational angles of the rods. Thus, b is a dimensionless damping coefficient, λ is a dimensionless follower force, and δ is an amplitude of the dimensionless noise $p(\tau)$. Then the equations of motion for the system of rods are

$$2x'' + y'' \cos(x-y) + (y')^2 \sin(x-y) + b(x' - y') \\ + 2x - y - \lambda \sin(x-y) = \delta p \cos y \quad (3a)$$

$$x'' \cos(x-y) + y'' - (x')^2 \sin(x-y) - b(x' - y') \\ - x + y = \delta p \cos y \quad (3b)$$

Here $p(\tau)$ is a periodic function with period $2\pi/\Omega$. The perturbed problem consists of determining periodic solutions of Eqs. (1) and (3) that possess the same period as the forcing function $p(\tau)$; that is

$$u(\tau + 2\pi/\Omega) = u(\tau) \quad \text{for all } \tau \quad (4)$$

where $u(\tau)$ is the vector with components x and y . For simplicity of presentation, the perturbed problem is expressed in the compact form

$$F[u, \lambda, \Omega, \delta] = 0 \quad (5)$$

The dependence of the perturbed problem on τ and the parameter b is not explicitly shown in Eq. (5).

The equations of motion (3) can be derived¹² by forming the Lagrangian of the mechanical system shown in Fig. 2. Linearized versions of Eqs. (3) with $p=0$ have been employed³⁻⁵ in previous stability studies.

III. Bifurcation (Flutter) Problem—Linear Theory

The bifurcation problem is obtained by setting $\delta=0$ and $\Omega=\omega$ in Eqs. (3) and (4). Here ω is the frequency of the solutions of the bifurcation problem to be determined. By employing the notation of Eq. (5), the bifurcation problem is expressed as

$$F[u, \lambda, \omega, 0] = 0 \quad (6a)$$

Since Eq. (6a) is translationally invariant in τ , the time axis is shifted to normalize the solutions by the condition

$$y'(0) = 0 \quad (6b)$$

The bifurcation problem, Eqs. (6), corresponds to the free oscillations of the nonconservative mechanical system. We wish to emphasize that condition (6b) cannot be imposed on the solutions of the perturbed problem.

The vertical, collinear state of the rods

$$u = u_0(\tau, \lambda, \omega) \equiv 0 \quad (7)$$

is a solution of Eqs. (6) for all values of λ and ω . It is the basic solution of the bifurcation problem.

The stability of the basic solution is determined from the linear bifurcation theory. It is obtained by linearizing Eqs. (3) and (4), with $\delta=0$, about the basic solution, Eq. (7). In the compact notation, Eqs. (6), the linear theory is expressed as

$$F_u[0, \lambda, \omega, 0]\varphi = 0, \quad \varphi'_2(0) = 0 \quad (8)$$

where $\varphi(t)$ is a vector with the components $\varphi_1(\tau)$ and $\varphi_2(\tau)$. The differential equations in Eq. (8) are linear with constant coefficients. Thus, they have solutions in the form

$$\varphi = ae^{\sigma\tau} \quad (9)$$

This leads to the stability equation

$$\sigma^4 + 5b\sigma^3 + 2(3-\lambda)\sigma^2 + b\sigma + 1 = 0 \quad (10)$$

The Routh-Hurwitz criteria applied to Eq. (10) show that the real parts of its four roots, $\sigma_j(\lambda)$, $j=1,2,3,4$ are negative if $\lambda < \lambda_c = 2/5$. Furthermore, we conclude that

$$\sigma_1(\lambda_c) = -\sigma_2(\lambda_c) = i\omega_0, \quad \omega_0 \equiv (5)^{-1/2} \quad (11)$$

$$\text{Re}\sigma_1(\lambda) > 0, \quad \text{Re}\sigma_2(\lambda) > 0, \quad \text{for } \lambda > \lambda_c \quad (12)$$

Application of the argument principle for analytic functions¹⁴ shows that $\text{Re}\sigma_{3,4}(\lambda) > 0$ for all λ . Thus, the basic solution is stable for $\lambda < \lambda_c$, neutrally stable for $\lambda = \lambda_c$, and unstable for $\lambda > \lambda_c$. The critical value λ_c corresponds to the critical flutter speed in panel flutter. A brief discussion of the dependence of λ_c on b is given in Appendix A.

The solutions of Eq. (8), evaluated at $\lambda = \lambda_c$, are a linear combination of the vectors $\varphi_1(\omega_0\tau)$ and $\varphi_2(\omega_0\tau)$. These vectors are defined by

$$\varphi_1(t) \equiv a \begin{bmatrix} C_1 \cos t - C_2 \sin t \\ \cos t \end{bmatrix}, \quad \varphi_2(t) \equiv \varphi_1(t - \pi/2) \quad (13)$$

The constants C_1 , C_2 , and a are defined by

$$C_1 \equiv \frac{5b^2 - 24}{25b^4 + 36}, \quad C_2 \equiv \frac{50b^2}{25b^4 + 36}, \quad a^2 \equiv \frac{2}{1 + C_1^2 + C_2^2} \quad (14)$$

To interpret the modal vectors in Eq. (13), we express them in phase-amplitude form

$$\varphi_1(t) = a \begin{bmatrix} C \cos(t + \zeta) \\ \cos t \end{bmatrix}, \quad \varphi_2(t) = \varphi_1(t - \pi/2) \quad (15)$$

Thus, C and ζ are the relative amplitude and phase angle of the response of the upper rod. They are defined by

$$C \equiv (C_1^2 + C_2^2)^{1/2}, \quad \tan \zeta \equiv C_2/C_1 \quad (16)$$

For small values of b , it follows from Eqs. (14) and (16) that

$$C \approx 2/3, \quad \zeta \approx \tan^{-1} \left(-\frac{25}{12} b^2 \right) \approx \pi \quad (17)$$

Thus, for small damping, the amplitude of the upper rod is smaller than the lower rod, and it is 180 deg out of phase with the lower rod. The smaller amplitude is consistent with the absence of friction at the lower point. For large values of b ,

$$C \approx 2/b^2, \quad \zeta \approx \tan^{-1} 10 \approx 1.47 \approx 84 \text{ deg} \quad (18)$$

Consequently, the amplitude of the upper rod is small, so that it remains nearly vertical while the lower rod oscillates. This results from the large damping in the common pivot.

IV. Bifurcation Problem—Nonlinear Theory

The Poincaré-Lindstedt perturbation method⁶ is now applied to obtain the periodic solutions of the bifurcation problem, Eqs. (6), that branch from the basic solution at $\lambda = \lambda_c$. The period, $2\pi/\omega$, of these solutions is to be determined. The existence of these solutions is guaranteed by the Hopf bifurcation theorem.

According to the Poincaré-Lindstedt method, a new time variable t is defined by

$$t = \omega \tau \quad (19)$$

In addition, an amplitude for the solutions is defined by

$$\epsilon^2 \equiv \langle u, u \rangle \quad (20)$$

Here, the inner product $\langle u_1, u_2 \rangle$ of any two vectors u_1 and u_2 is

$$\langle u_1, u_2 \rangle \equiv \frac{1}{2\pi} \int_0^{2\pi} (u_1(t), u_2(t)) dt \quad (21)$$

where the notation $(u_1(t), u_2(t))$ indicates the usual dot product of two vectors. Then we seek solutions of Eqs. (6) by expanding u , λ , and ω in power series in ϵ near the critical value $u=0$, $\lambda=\lambda_c$, and $\omega=\omega_0$. Omitting all details of the calculations, this gives

$$u = \epsilon \varphi_1 + O(\epsilon^3) \quad (22a)$$

$$\lambda(\epsilon) = \lambda_c + \lambda_2 \epsilon^2/2 + O(\epsilon^4) \quad (22b)$$

$$\omega(\epsilon) = \omega_0 + \omega_2 \epsilon^2/2 + O(\epsilon^4) \quad (22c)$$

The vector φ_1 , which is defined in Eq. (15), and the constants λ_2 and ω_2 , are given by

$$\lambda_2 = \frac{1}{3\Delta} \{ -\langle F_{u\lambda}^0 \varphi_1, \psi_2 \rangle \langle F_{uuu}^0 \varphi_1^3, \psi_1 \rangle + \langle F_{u\omega}^0 \varphi_1, \psi_1 \rangle \langle F_{uuu}^0 \varphi_1^3, \psi_2 \rangle \}$$

$$\omega_2 = \frac{1}{3\Delta} \{ -\langle F_{u\lambda}^0 \varphi_1, \psi_1 \rangle \langle F_{uuu}^0 \varphi_1^3, \psi_2 \rangle + \langle F_{u\omega}^0 \varphi_1, \psi_2 \rangle \langle F_{uuu}^0 \varphi_1^3, \psi_1 \rangle \} \quad (23)$$

A superscript 0 on the operator F and its derivatives in Eq. (23) signify the operator evaluated at the critical point $u=0$, $\lambda=\lambda_c$, and $\omega=\omega_0$. The vectors ψ_1 and ψ_2 , and the scalar Δ are defined by

$$\psi_1 \equiv \frac{1}{\sqrt{2}} \begin{bmatrix} \cos t \\ \cos t \end{bmatrix}, \quad \psi_2 \equiv \psi_1(t - \pi/2) \quad (24)$$

$$\Delta \equiv \langle F_{u\lambda}^0 \varphi_1, \psi_1 \rangle \langle F_{u\omega}^0 \varphi_1, \psi_2 \rangle - \langle F_{u\omega}^0 \varphi_1, \psi_1 \rangle \langle F_{u\lambda}^0 \varphi_1, \psi_2 \rangle \quad (25)$$

The vectors in Eq. (24) span the null space of the operator that is the adjoint of the linearized operator F_u^0 .

The perturbation calculations that lead to Eqs. (22) and (23) are standard, but they are exceedingly complex algebraically. To circumvent this difficulty we employed the computer symbolic manipulation language ALTRAN.¹¹ It symbolically performs the algebraic manipulations of the perturbation methods used in this section and in Sec. V. It was used to algebraically manipulate truncated power series, to differentiate polynomials, and to solve symbolically linear systems of algebraic equations. It would have been difficult to perform the perturbation calculations without the aid of ALTRAN. In addition, useful relations among the algebraic expressions such as symmetries or common factors were discovered by the automatic simplifications performed by ALTRAN. Some of these useful symmetries are listed in Appendix B.

As a result of the manipulations by ALTRAN, we obtain

$$\lambda_2 = \frac{425b^8 - 70b^6 + 1257b^4 - 72b^2 + 1296}{2Y} > 0$$

$$\omega_2 = \frac{15[(5b^4 - b^2 + 12)^2 + 100b^4]}{2\sqrt{5}Y} > 0$$

$$\Delta = \frac{100\sqrt{5}b^2(25b^4 + 36)}{Y} > 0 \quad (26)$$

where the quantity Y is defined by

$$Y(b) \equiv (25b^4 + 36)^2 + (5b^2 - 24)^2 + (50b^2)^2 > 0 \quad (27)$$

The positivity of λ_2 follows from an elementary analysis of the numerator of its expression in Eq. (26). Since $\lambda_2 > 0$, it then follows from Eq. (22b) that a unique periodic solution of Eqs. (6) bifurcates supercritically from the critical value λ_c . Furthermore, since $\omega_2 > 0$, the frequency increases with the amplitude. Thus, the mechanical system responds like a "stiff" spring. The solution, Eqs. (22), corresponds to the flutter state for the panel.

Equations (22) yield a response curve in λ , ω , and ϵ space. This curve emanates from the critical point, $\lambda=\lambda_c$, $\omega=\omega_0$, and $\epsilon=0$. Its projection onto the plane $\omega=\omega_0$ gives the amplitude response diagrams discussed in Sec. I; see the dotted curve in Fig. 1.

V. Perturbed Bifurcation Problem

Asymptotic expansions as $\delta \rightarrow 0$ of the solutions of the perturbed problem (5) are obtained as perturbations of the bifurcation solutions. These perturbations are singular in the parameter λ as $\lambda \rightarrow \lambda_c$. The method of matched asymptotic expansions was employed in Refs. 7 and 8 to analyze such singular perturbations of bifurcation. A generalization of this method is used in this section; a brief summary of this method

is now presented. All details of the calculations are omitted because of their substantial length, algebraic complexity, and because there have been several previous applications of the method.⁷⁻¹⁰

Let $u_0(\lambda)$ denote any of the four solutions of the bifurcation problem in Eqs. (6) that branch from λ_c (see Fig. 1). Then we seek asymptotic expansions of the solutions of the perturbed problem in the form

$$u(\lambda, \Omega(\lambda), \delta) = u(\lambda, \delta) = u_0(\lambda) + \sum_{j=1}^{\infty} u_j(\lambda) \delta^j \quad (28)$$

By inserting Eq. (28) into Eq. (5), we find that the coefficients u_j , $j=1, 2, \dots$, satisfy inhomogeneous linear problems. It can be shown that the solutions of these problems are unbounded as $\lambda \rightarrow \lambda_c$, since the imperfections are assumed to satisfy the condition

$$I^2 \equiv I_1^2 + I_2^2 \neq 0 \quad (29a)$$

The imperfection parameters I_1 and I_2 are defined by

$$I_j \equiv \langle F_\delta[0, \lambda_c, \omega_0, 0], \psi_j \rangle \quad j=1, 2 \quad (29b)$$

Thus, the expansions in Eq. (28) are not valid as $\lambda \rightarrow \lambda_c$; they are called the outer expansions. Since the components of the vector $F_\delta[0, \lambda_c, \omega_0, 0]$ are proportional to $-p(t)$, Eq. (29a) is equivalent to

$$8\pi^2 I^2 = \left[\int_0^{2\pi} p(t) \cos t dt \right]^2 + \left[\int_0^{2\pi} p(t) \sin t dt \right]^2 \neq 0 \quad (30)$$

If Eq. (30) is violated, then bifurcation may not be destroyed by the disturbance $p(t)$. See Ref. 8 for a discussion of weak imperfections.

Asymptotic expansions of the solutions of the perturbed problem that are valid near $\lambda = \lambda_c$ are obtained in the form

$$u(\lambda(\mu), \delta(\mu)) = \sum_{j=0}^{\infty} z_j \mu^j \quad (31a)$$

$$\lambda = \lambda(\mu) = \lambda_c + \xi \mu^2 / 2 + O(\mu^3) \quad (31b)$$

$$\delta = \delta(\mu) \equiv (\text{sgn} \delta) \mu^3 \quad (31c)$$

They are the inner expansions. The new small parameter μ is defined by Eq. (31c) and ξ is the inner or boundary-layer variable. Then Eqs. (1) and (31b) imply that near $\lambda = \lambda_c$ we have

$$\Omega = \omega_0 + w \xi \mu^2 / 2 + O(\mu^3) \quad (32)$$

By inserting Eqs. (31) into Eq. (5) we obtain, in the usual way, a sequence of linear problems to determine the coefficients z_j . An analysis of these problems gives

$$z_1 = A \varphi_1 + B \varphi_2 \quad (33)$$

where φ_1 and φ_2 are defined in Eq. (15). The constants A and B are solutions of a system of two nonlinear algebraic equations. These equations are expressed in a more tractable form by first defining polar coordinates ρ and α by

$$A = \rho \cos \alpha, \quad B = \rho \sin \alpha \quad (34)$$

Then, by inserting Eq. (34) into these algebraic equations, and taking appropriate linear combinations of the result, the

algebraic equations are reduced to

$$\left[-\frac{\beta}{\Delta_1} \rho^3 + \xi \rho \right] \cos \alpha + \frac{\Delta}{\Delta_1} (\omega_2 - w \lambda_2) \rho^3 \sin \alpha = (\text{sgn} \delta) \frac{A_1}{3} \quad (35a)$$

$$-\frac{\Delta}{\Delta_1} (\omega_2 - w \lambda_2) \rho^3 \cos \alpha + \left[-\frac{\beta}{\Delta_1} \rho^3 + \xi \rho \right] \sin \alpha = (\text{sgn} \delta) \frac{A_2}{3} \quad (35b)$$

The quantities ω_2, λ_2 , and Δ are given in Eq. (26). The coefficients β, Δ_1, A_1 , and A_2 are defined in terms of the quantities

$$D_{ij} \equiv \langle F_{u\lambda}^0 \varphi_i, \psi_j \rangle, \quad E_{ij} \equiv \langle F_{u\Omega}^0 \varphi_i, \psi_j \rangle \quad (36)$$

by

$$\beta \equiv (D_{11}^2 + D_{12}^2) \lambda_2 + (E_{11}^2 + E_{12}^2) w \omega_2$$

$$\Delta_1 \equiv (D_{11} + w E_{11})^2 + (D_{12} + w E_{12})^2 > 0$$

$$\Delta_1 A_1 \equiv (D_{11} + w E_{11}) I_1 + (D_{12} + w E_{12}) I_2$$

$$\Delta_1 A_2 \equiv -(D_{12} + w E_{12}) I_1 + (D_{11} + w E_{11}) I_2 \quad (37)$$

The expressions for the quantities in Eq. (36) that were obtained using ALTRAN are listed in Appendix C.

The linear equation to determine z_1 is $F_u[0, \lambda_c, \omega_0, 0] z_1 = 0$. Its general solution, Eq. (33), is a linear combination of the two independent solutions, φ_1 and φ_2 . The method, as presented in Refs. 7 and 8, assumes that this linear problem has only one independent solution. The present generalization is only slight. Nevertheless, substantially different results are obtained, as we demonstrate in Sec. VI.

For each real root $[\rho(\xi), \alpha(\xi)]$ of the amplitude equations (35), we obtain from Eqs. (31), (33), (34), and (15) an inner expansion

$$u = a \rho \begin{bmatrix} C \cos(t + \xi - \alpha) \\ \cos(t - \alpha) \end{bmatrix} \delta^{1/3} + O(\delta^{2/3}) \quad (38)$$

Thus, we refer to ρ as the amplitude of the response. If $p(t) = \cos t$, then α represents a phase shift in the response. The upper rod is phase shifted with respect to the lower rod by an angle ξ , as we discussed in Sec. III. The matching conditions of the method of matched asymptotic expansions⁶ are then used to determine how the various inner and outer expansions "connect" (see the discussion in Ref. 7). Finally, the composite expansions of the method then give asymptotic expansions of the solution of the perturbed problem that are uniformly valid in λ .

Thus, from the matching conditions, we obtain the following conclusions. If $w \neq w^0$, where w^0 is defined by

$$w^0 \equiv \omega_2 / \lambda_2 \quad (39)$$

then $\rho \rightarrow 0$ as $|\xi| \rightarrow \infty$; that is, the inner expansions match with the outer expansions corresponding to the two branches of the basic solution. If $w = w^0$, then the inner expansions match with the outer expansions corresponding to the bifurcated (basic) states as $\xi \rightarrow \infty (-\infty)$.

To interpret Eq. (39) we insert it into Eq. (1) to give the forcing frequency as

$$\Omega = \omega_0 + (\omega_2 / \lambda_2) (\lambda - \lambda_c) + O((\lambda - \lambda_c)^2) \quad (40)$$

However, by eliminating ϵ^2 from the representation, Eqs. (22b) and (22c) of the bifurcated state, we get

$$\omega = \omega_0 + (\omega_2/\lambda_2)(\lambda - \lambda_c) + O((\lambda - \lambda_c)^2) \quad (41)$$

Hence, we conclude from Eqs. (40) and (41) that Eq. (39) implies that the impressed frequency equals the response frequency of the bifurcated state to $O((\lambda - \lambda_c)^2)$.

VI. Analysis of the Amplitude Equations

The amplitude equations are analyzed first for the special case $w = w^0$. Then, by squaring Eqs. (35), and adding the results, we obtain the following two cubics for the amplitude ρ :

$$\rho^3 - \frac{\Delta_1}{\beta} \xi \rho \pm \frac{\Delta_1}{3} (A_1^2 + A_2^2)^{1/2} = 0 \quad (42)$$

Similar cubic equations were obtained previously.^{7,8} A sketch of the variation of ρ with λ is shown by the solid curve in Fig. 3f, where we have used the relationship between ξ and λ given by Eq. (31b). Equations (37) imply that $A_1 = A_2 = 0$ when $I_1 = I_2 = 0$. Then the roots of Eq. (42) give the basic and bifurcated solutions. The bifurcated solution is shown by the dotted curve in the figure. Thus, when $w = w^0$ the roots of Eq. (42) give the smooth transition from the basic to the flutter state as λ increases.

To solve Eqs. (35) in the general case when $w \neq w^0$, we observe that the amplitude equations are linear in $\cos \alpha$ and $\sin \alpha$, and that

$$A_1^2 + A_2^2 \neq 0 \quad (43a)$$

The condition of Eq. (43a) follows directly from Eq. (29), the definitions of A_1 and A_2 in Eqs. (37), and from the inequality $\Delta > 0$. Since $w \neq w^0$, the determinant γ of Eqs. (35) as a linear system for $\cos \alpha$ and $\sin \alpha$ vanishes if, and only if, $\rho = 0$. However, if $\rho = 0$, then Eqs. (35) imply that $A_1 = A_2 = 0$, which violates Eq. (43). Thus, Eqs. (35) can be solved uniquely. This gives

$$\cos \alpha = \frac{(\text{sgn} \delta)}{3\gamma} \rho \left\{ \left(-\frac{\beta}{\Delta_1} \rho^2 + \xi \right) A_1 - \frac{\Delta}{\Delta_1} (\omega_2 - w\lambda_2) \rho^2 A_2 \right\} \quad (43b)$$

$$\sin \alpha = \frac{(\text{sgn} \delta)}{3\gamma} \rho \left\{ \frac{\Delta}{\Delta_1} (\omega_2 - w\lambda_2) \rho^2 A_1 + \left(-\frac{\beta}{\Delta_1} \rho^2 + \xi \right) A_2 \right\} \quad (43c)$$

where γ is defined by

$$\gamma = \rho^2 \left\{ \left(-\frac{\beta}{\Delta_1} \rho^2 + 3\xi \right)^2 + \left[\frac{\Delta}{\Delta_1} (\omega_2 - w\lambda_2) \rho^2 \right]^2 \right\} \quad (43d)$$

An equation for ρ only is obtained by eliminating α from Eqs. (43b) and (43c). This gives the sixth degree polynomial equation

$$\left[\frac{\Delta}{\Delta_1} (\omega_2 - w\lambda_2) \right]^2 \rho^6 + \left[-\frac{\beta}{\Delta_1} \rho^2 + \xi \right]^2 \rho^2 - \left[\frac{A_1^2 + A_2^2}{9} \right] = 0 \quad (44)$$

Corresponding to each real root $\rho(\xi)$ of Eq. (44), a value of $\alpha(\xi)$ is obtained from Eqs. (43b), (43c), and (43d), and an

inner expansion from Eq. (38). This can then be combined with the outer expansions to obtain uniform, composite expansions of the solutions of the perturbed problem.

The qualitative properties of the real roots of Eq. (44) are obtained by first solving for $\xi = \xi(\rho, w)$. This gives

$$\xi = (\beta/\Delta_1) \rho^2 \pm \rho^{-1} (A^2 - k^2 \rho^6)^{1/2} \quad (45)$$

where we have used the following notation:

$$A \equiv \left(\frac{A_1^2 + A_2^2}{3} \right)^{1/2}, \quad k \equiv \frac{\Delta}{\Delta_1} (\omega_2 - w\lambda_2) \quad (46)$$

It follows directly from Eq. (45) that the real roots are bounded above by

$$\rho = \rho_m \equiv (A/k)^{1/2} \quad (47)$$

The corresponding value of ξ , which we call ξ_m , is obtained from Eq. (45) as

$$\xi_m = (\beta/\Delta_1) \rho_m^3 \quad (48)$$

Thus, the response curves, $\rho = \rho(\lambda)$, for the solutions of the perturbed problem, have a local maximum at $\lambda = \lambda_m \equiv \lambda_c + \xi_m \delta^{1/2} + O(\delta)$, $\rho = \rho_m$. The position of the maximum varies as w varies, because β depends on w [see Eq. (37)].

The qualitative features of the roots depend on the values of w , and on the magnitude of the parameter

$$q \equiv \frac{3^{1/2} \Delta \lambda_2}{E^2 \omega_2}, \quad E^2 \equiv E_{11}^2 + E_{12}^2 = \frac{10b^4 (100b^4 + 60b^2 + 909)}{Y} \quad (49)$$

From ALTRAN, we obtain

$$q = 5\sqrt{3} [10625b^{12} - 1750b^{10} + 46725b^8 - 77652b^6 - 2592b^2 + 46656] / 3b^2 [2500b^{12} + 500b^{10} + 44225b^8 + 1770b^6 + 213849b^4 - 13176b^2 + 130896] \quad (50)$$

If $q > 1$, then an elementary analysis of Eq. (45), which we do not present, shows that in addition to w^0 there are three other critical values of w . They are defined by

$$w^1 \equiv -\frac{D^2 \lambda_2}{E^2 \omega_2} < 0, \quad D^2 \equiv D_{11}^2 + D_{12}^2, \quad w^\pm \equiv \frac{3^{1/2} \Delta w^0 \pm D^2}{3^{1/2} \Delta \mp E^2 w^0} \quad (51)$$

The response diagrams in the four regions that are determined by Eqs. (51) are shown in Fig. 3. The dotted curve in each of these figures is the state that bifurcates from $\lambda = \lambda_c$. It is obtained from Eqs. (22) by expressing ϵ in terms of ρ .

The significance of the critical value w^1 is that $\lambda_m < \lambda_c (> \lambda_c)$ if $w < w^1 (> w^1)$. At $w = w^1$, λ_m coincides with λ_c . Furthermore, the critical values w^+ and w^- determine an interval $w^- < w < w^+$, in which the amplitude is a multivalued function of λ , as shown in the figures. As $w \rightarrow w^0$, the maximum amplitude $\rightarrow \infty$, as we deduce from Eq. (39), and the definition of k in Eq. (46). At $w = w^-$ and $w = w^+$, the amplitude has a vertical slope at $\lambda = \lambda_m$.

A new critical value $w = w^*$ occurs if $q < 1$. It is defined by

$$w^* \equiv \frac{D^2 - 3^{1/2} \Delta w^0}{3^{1/2} \Delta - E^2 w^0} \quad (52)$$

If w lies in the interval, $w^* < w < w^-$, the amplitude is a single-valued function of λ with a single maximum. The maximum occurs to the left (right) of λ_c if w is in $w^* < w < w^l$ ($w^l < w < w^-$). For any values of w outside $[w^*, w]$, the response is multivalued. Response curves similar to Fig. 3, when $q < 1$, are not shown.

VII. Discussion of Results

Each point on the solid curves in Fig. 3 represents a small-amplitude, time-periodic solution of the perturbed problem. These solutions have the same period as the disturbance $p(\tau)$. They are perturbations of the basic solution. Hence, we refer to them as weak flutter states. They have a maximum amplitude at $\lambda = \lambda_m$. The values of this maximum, and its location, depend on the impressed frequency Ω and the imperfection parameters I_1 and I_2 . As $w \rightarrow w^0 \equiv \omega_2/\lambda_2$, $\rho_m \rightarrow \infty$, and $\lambda_m \rightarrow \infty$, as we deduce from Eqs. (45-48). That is, at $w = w^0$, the amplitude of the weak flutter state does not have a local maximum. It represents a smooth transition from the basic state to the flutter (bifurcation) state, as is shown in Fig. 3f.

The interpretation of the results depends on the stability of the solutions. We assume, as is usually the case, that a solution is stable (unstable) if

$$\frac{d\rho}{d\lambda} > 0 (< 0) \quad (53)$$

That is, it is stable if the amplitude of the response increases as the magnitude of the input (flow velocity) λ increases. It is unstable if the converse is true. Although this assumption is physically reasonable, it should be verified mathematically from linear stability theory. We do not give this verification.

Referring to Fig. 3, we observe that as λ increases from zero, the rods oscillate in a weak flutter state. If $w \neq w^0$, the amplitudes of these oscillations increase until $\lambda = \lambda_m$. Any further increase in λ results in an unstable solution. This suggests that as λ increases through λ_m , there is a dynamic transition to another state. This transition may be rapid and involve large amplitudes. Specifically, if w is in the interval, $w^- < w < w^+$, the response is multivalued, as shown in Fig. 3e. Then for $\lambda = \lambda_m$, the solutions may execute a "small" jump from the upper branch with $\rho = \rho_m$, to the stable intermediate branch with $\rho = \rho_f$. Then by increasing λ further, a second transition will occur at $\lambda = \lambda_u$ with a relatively large jump to some other solution. However, if λ is decreased from λ_m after the jump to the intermediate branch, a second transition will occur at $\lambda = \lambda_l$. The solution may jump to the upper branch or to some other solution. If w lies outside the interval $w^- < w < w^+$, then at $\lambda = \lambda_m$ and $\rho = \rho_m$, there are no stable, nearby, periodic solutions. This implies a dynamic transition, possibly with large amplitudes.

The results show that unless $w = w^0$, the periodic disturbance does not provide a smooth transition to the flutter state. Rather, it introduces the possibility of a jump transition at the new critical value $\lambda = \lambda_m$. We observe from Fig. 3a that if $w < w^l$, then $\lambda_m < \lambda_c$. This implies that if the frequency of the disturbance varies so that $w < w^l$, then early transition is induced at $\lambda = \lambda_m < \lambda_c$. Conversely, if w exceeds w^l , so that λ_m exceeds λ_c , then transition is delayed until $\lambda = \lambda_m > \lambda_c$. Additional transitions may occur if w is in the interval (w^-, w^+) .

The present analysis determines periodic solutions near the basic solutions and of the same frequency as the disturbance. However, there may be other periodic and nonperiodic solutions of the perturbed problem. The significance of these solutions and all the other solutions of the initial value problem corresponding to the differential equations (3) depends on their stabilities. Since the long-time response of the initial value problem is not yet known, it is difficult to assess the significance of these additional solutions.

The stability of the mechanical system depends on two competing effects. The horizontal force p disturbs the rods from their vertical equilibrium state. This tends to destabilize the rods. However, the resulting response is phase shifted by an angle α , as we observe in Eq. (38). If the phase shift is small, the disturbance effect of the force wins, and early transition occurs as in Figs. 3a and 3b. However, if the phase shift is sufficiently large, then the restraining effect of the horizontal force wins, and transition is delayed, as in Figs. 3c-e, 3g, and 3h. An analysis of Eqs. (43) for α , which we do not present, confirms these remarks.

Disturbances frequently consist of a continuous spectrum of frequencies. If the spectrum "peaks" at distinct frequencies, as experiments suggest in panel flutter, then the present analysis applied to periodic disturbances with these peak frequencies may provide an approximation to the response. Generalizations of the present method to nonperiodic disturbances are presently under investigation.

An alternate interpretation of these results is obtained if $p(\tau)$ is considered as a specified forcing function. Then the results suggest that the transition to flutter can be controlled by appropriately specifying the variation with λ of the forcing function. In particular, the transition can be delayed by applying a forcing function with $w > w^l$. This interpretation may be of practical significance for the control of panel flutter. Additional control might be achieved, for example, by applying a similar horizontal periodic force at the middle pivot between the rods, with this force phase shifted with respect to the horizontal force at the tip.

Appendix A—Remarks on the Effects of Damping

The critical value $\lambda_c = 2/5$ is independent of b . However, if $b = 0$ in Eq. (10), the resulting stability equation is biquadratic. Hence, it can be solved explicitly. Then the critical value is $\lambda_c = 2$ and λ_c is not a continuous function of b for b near $b = 0$.

To clarify this point further, the original mechanical system is modified by allowing the lower pivot to have damping proportional to θ' , with dimensionless damping coefficient b_1 . Then the resulting critical value of λ_c is given by

$$\lambda_c(b, b_1) = 2 \left[\frac{b_1^2 + 6bb_1 + b^2}{b_1^2 + 6bb_1 + 5b^2} \right] + \frac{bb_1}{2} \quad (A1)$$

The behavior of λ_c as b and b_1 approach zero depends explicitly on how these two parameters approach zero. For example if we set $b = \alpha b_1$, for a fixed α , and then let $b_1 \rightarrow 0$, we obtain different values of $\lambda_c(0, 0)$ depending on the value of α . Thus, $\lambda_c(b, b_1)$ is not a continuous function near the origin of the b_1, b plane. Further consequences of this discontinuous behavior with regard to the destabilizing effects of damping are discussed elsewhere.^{12,15,16}

Appendix B—Symmetries of the Bifurcation Problem

The bifurcation problem, Eq. (6), satisfies the following identities:

$$\langle F_{ua}^0 \phi_2, \psi_1 \rangle = -\langle F_{ua}^0 \phi_1, \psi_2 \rangle, \quad \langle F_{ua}^0 \phi_2, \psi_2 \rangle = \langle F_{ua}^0 \phi_1, \psi_1 \rangle$$

$$a = \lambda, \omega$$

$$3P_{1122} = 3P_{1221} = P_{2222} = P_{1111}$$

$$-3P_{1121} = 3P_{1222} = -P_{2221} = P_{1112}$$

where the quantities P_{ijkl} are defined by

$$P_{ijkl} \equiv \langle (F_{uuu}^0 \phi_i) \phi_j \rangle \phi_k, \psi_l \rangle$$

Appendix C—Coefficients and Parameters in the Inner Expansions

The quantities in Eq. (36) are given explicitly by

$$Y^{1/2} D_{11} = 5(5b^4 - b^2 + 12), \quad Y^{1/2} D_{12} = 50b^2$$

$$Y^{1/2} E_{11} = 2\sqrt{5}b^2(10b^3 + 3), \quad Y^{1/2} E_{12} = 60\sqrt{5}b^2$$

Acknowledgments

The research reported in this paper was supported by the U. S. Air Force Office of Scientific Research under Grant AFOSR 80-0016. All computations were performed at the Department of Energy Computing and Applied Mathematics Center at New York University. The results in this paper form part of the thesis of L. R. Sinay submitted in partial fulfillment of the requirements for the Ph.D. at New York University, 1978.

References

- ¹Dowell, E. H., *Aeroelasticity of Plates and Shells*, Noordhoff Publishing, Leyden, 1975.
- ²Muhlstein, L., Gaspers, P. A., and Riddle, D. W., "An Experimental Study of the Influence of the Turbulent Boundary Layer on Panel Flutter," NASA TND-4486, 1968.
- ³Bolotin, V. V., *Nonconservative Problems of the Theory of Elastic Stability*, Pergamon Press, Oxford, 1963.
- ⁴Herrmann, G., "Dynamics and Stability of Mechanical Systems with Follower Forces," NASA CR-1782, Nov. 1971.
- ⁵Ziegler, H., *Principles of Structural Stability*, Blaisdell, Waltham, Mass., 1968.
- ⁶Cole, J., *Perturbation Methods in Applied Mathematics*, Blaisdell, Waltham, Mass., 1968, pp. 82-86, and 4-26.
- ⁷Matkowsky, B. J. and Reiss, E. L., "Singular Perturbations of Bifurcation," *SIAM Journal on Applied Mathematics*, Vol. 33, Sept. 1977, pp. 230-255.
- ⁸Reiss, E. L., "Imperfect Bifurcation," *Applications of Bifurcation Theory*, Academic Press, New York, 1977, pp. 37-71.
- ⁹Tavantzis, J., Reiss, E. L., and Matkowsky, B. J., "On the Smooth Transition to Convection," *SIAM Journal on Applied Mathematics*, Vol. 34, March 1978, pp. 322-337.
- ¹⁰Watson, J. G. and Reiss, E. L., "A Statistical Theory of Imperfect Bifurcation," *SIAM Journal on Applied Mathematics*, in press.
- ¹¹Brown, W. S., *ALTRAN User's Manual*, 4th Ed., Bell Laboratories, Murray Hill, N. J., 1977.
- ¹²Sinay, L., "Nonlinear Stability of a Two-Degree-of-Freedom, Non-Conservative, Mechanical System," Ph.D. Thesis, Courant Institute of Mathematical Sciences, New York University, May 1978.
- ¹³Strumolo, G. and Reiss, E. L., "Poiseuille Channel Flow with Driven Walls," submitted *Journal of Fluid Mechanics*.
- ¹⁴Markushevich, A. I., *Theory of Functions of a Complex Variable*, Chelsea Publishing Co., New York, 1977.
- ¹⁵Sinay, L., "Kelvin's Destabilizing Effect of Small Damping," *Seminar on Numerical Analysis and its Applications to Continuum Physics*, coleção atas da Brazilian Mathematical Society, Vol. 12, 1980, pp. 21-27.
- ¹⁶Sinay, L., "Destabilizing Effect of Small Damping," *Atas do 10^o Seminario de Analise*, Brazilian Mathematical Society, 1979, pp. 178-196.

From the AIAA Progress in Astronautics and Aeronautics Series . . .

INJECTION AND MIXING IN TURBULENT FLOW—v. 68

By Joseph A. Schetz, Virginia Polytechnic Institute and State University

Turbulent flows involving injection and mixing occur in many engineering situations and in a variety of natural phenomena. Liquid or gaseous fuel injection in jet and rocket engines is of concern to the aerospace engineer; the mechanical engineer must estimate the mixing zone produced by the injection of condenser cooling water into a waterway; the chemical engineer is interested in process mixers and reactors; the civil engineer is involved with the dispersion of pollutants in the atmosphere; and oceanographers and meteorologists are concerned with mixing of fluid masses on a large scale. These are but a few examples of specific physical cases that are encompassed within the scope of this book. The volume is organized to provide a detailed coverage of both the available experimental data and the theoretical prediction methods in current use. The case of a single jet in a coaxial stream is used as a baseline case, and the effects of axial pressure gradient, self-propulsion, swirl, two-phase mixtures, three-dimensional geometry, transverse injection, buoyancy forces, and viscous-inviscid interaction are discussed as variations on the baseline case.

200 pp., 6×9, illus., \$17.00 Mem., \$27.00 List

TO ORDER WRITE: Publications Dept., AIAA, 1290 Avenue of the Americas, New York, N. Y. 10019